Communication in Physical Sciences 2021, 7(3): 182-202

Synthesis, Spectroscopic, Biological and DFT Studies of 2,4,6-Tris(4-Carboxyphenylimino-4[1]-Formylphenoxy)-1,3,5-Triazine and its Trinuclear Dy(III) and Er(III) Salen Capped Complexes

Uchechukwu S. Oruma, Pius O. Ukoha, Collins U. Ibeji, Lawrence N. Obasi, Obinna C. Okpareke, Ebubechukwu N. Dim, Klaus Jurkschat and Ponnadurai Ramasami

Received 29 August 2021/Accepted 23 September 2021/Published online: 27 September 2021

Abstract: *A tripodal Schiff base ligand, 2,4,6-tris(4-carboxyphenylimino-4[1]-formylphenoxy)-1,3,5-triazine (H_3CT) and its trinuclear Dy(III) and Er(III) complexes were synthesized. Characterization of these compounds was done via UV-Visible, IR, ^1H and ^{13}C NMR spectroscopies, elemental analysis and molar conductivity measurements. The spectral studies indicate that the ligand is hexadentate and coordinates to Dy/Er(III) ions through the oxygen atoms of the carboxylic group. The trinuclear complexes were characterized as being bridged by a carboxylic group to the Dy(III) and Er(III) salen centres and displays a coordination number of six. Biological studies revealed that the Dy(III) complex showed the highest activity against tested microorganisms and also gave the highest percentage parasitemia inhibition (84.0 %) relative to Artesunate (87.2 %). DFT calculations were carried out to enhance understanding of H_3CT at the molecular level based on (B3LYP)/6-31+G(d,p). The molecular docking results revealed the binding mode of H_3CT complexed with Staphylococcus aureus.*

Keywords: *Tripodal Schiff base; 1,3,5-triazine, trinuclearDy/Er(III) complexes; antimicrobial activity; antimalarial activity; DFT, docking*

Uchechukwu Susan Oruma*
Coordination Chemistry and Inorganic Pharmaceuticals Unit, Department of Pure and Industrial Chemistry, University of Nigeria, Nsukka, 410001, Nigeria.
Email: susan.oruma@unn.edu.ng
Orcid. Id: 0000-0002-9226-2512

Pius Oziri Ukoha
Coordination Chemistry and Inorganic Pharmaceuticals Unit, Department of Pure and Industrial Chemistry, University of Nigeria, Nsukka, 410001, Nigeria.
Email: pius.ukoha@unn.edu.ng
Orcid id: 0000-0003-3041-0919

Collins U. Ibeji
Catalysis and Peptide Research Unit, School of Health Sciences, University of KwaZulu-Natal, Durban 4041, South Africa,
Department of Pure and Industrial Chemistry, University of Nigeria, Nsukka, 410001, Nigeria.
Email: Ugochukwu.ibeji@unn.edu.ng
Orcid id: 0000-0003-4762-2256

Lawrence Nnamdi Obasi
Coordination Chemistry and Inorganic Pharmaceuticals Unit,
Department of Pure and Industrial Chemistry,
University of Nigeria, Nsukka, 410001, Nigeria.
Email:nnamdi.obasi@unn.edu.ng
Orcid id: 0000-0001-9310-0825

Obinna C. Okpareke
Department of Pure and Industrial Chemistry, University of Nigeria, Nsukka, 410001, Nigeria.
Email: Obinna.okpareke@unn.edu.ng

Ebubechukwu N. Dim
Department of Pure and Industrial Chemistry, University of Nigeria, Nsukka, 410001, Nigeria.
Email: Ebubechukwu.dim@unn.edu.ng

Klaus Jurkschat
Technische Universität, Fakultät für Chemie und Chemische Biologie, -44221 Dortmund, Germany.
Email: Klaus.jurkschat@tu-dortmunde.de

PonnaduraiRamasami
Computational Chemistry Group, Department of Chemistry, Faculty of Science, University of Mauritius, Réduit 80837, Mauritius.
Department of Applied Chemistry, University of Johannesburg, Doornfontein, Johannesburg 2028, South Africa.
Email: ramchemi@intnet.mu

1.0 Introduction

Tripodal ligands refer to those which have three arms containing donor atoms (N, S, P, or O) through which they can bind to one or more metals. They are generally employed in coordination, bioinorganic and organometallic chemistry in building multinuclear metal complexes (Kocyigit and Guler, 2010; Kocyigit 2013). These multinuclear metal complexes are related to multimetal active sites of various metalloproteins and metallo-enzymes (Hu *et al*., 2003). Examples of tripodal ligands are: triazine tripods, tripyridylalkylamine(TPA) tripods, polypyridylamine tripods (Kocyigit and Guler, 2010; Kocyigit 2013),t ris(2-aminoethyl)amine(tren) tripods, tris(2-pyridyl) tripods and tris(pyrazolyl)borate tripods. Substituted s-triazines derivatives have been known to possess anticancer (Afonso *et al.*, 2006; Kumar *et al.*, 2010; Sączewski *et al*., 2006), antitumor (Arya and Dandia, 2007; Bespalov *et al*., 2011; Zheng *et al*., 2007), antiviral (Lemke *et al*., 2010), and antifungal activities (Milata *et al*., 2012). They are used as bridging agents in the synthesis of herbicides, drugs or polymers (De Hoog *et al*., 2002; Uysal and Koc, 2010).

Tripodal- trinuclear [salen metal (III)] capped complexes of some main group and d-block metals have been synthesized and characterized, but no report exists of such complexes with the lanthanides. The work done by Koc and Ucan (Koc and Ucan, 2007) was the first reported synthesis of tripodal-trinuclear [salen metal (III)] capped complexes. There is no report on their applications in biological studies.

Salen (N,N^1-bis(salicylidene)ethylenediamine) has been recognized as one of the best known tetradentate organic ligands (Chen *et al.*, 2013; Yue *et al*., 2015) with an N_2O_2 cavity (Taha*et al*., 2011).Salen ligand was first synthesized by Jacobsen and Katsuki in 1990 when they discovered the enantioselective epoxidation of unfunctionalized alkenes using chiral Mn(salen) complexes (Irie *et al*., 1990; Zhang *et al.*, 1990). Salen-type ligands have been employed in the synthesis of numerous metal complexes, both with transition and non-transition metals (Chen *et al.*, 2013; DallaCort *et al*., 2010; Fei *et al*., 2016) and their complexes are of great interest in chemistry because of their catalytic activities in a wide range of useful organic transformations (Sathe *et al.*, 2013). Their ability to form ligand complexes has been used to obtain capped complexes (Uysal and Koç, 2016). Earlier studies (DallaCort*et al.*, 2010) implicated the metal centre of salen complexes as being responsible for most of the activities like catalysis, chiral synthesis and biological activities. Consequently, most lanthanide salen/salen-type complexes have been employed in luminescent study (Chen *et al*., 2013; Yue *et al.*, 2015; Taha *et al*., 2011; Cristóvão and Hnatejko, 2015) and magnetic study (Chien *et al*., 2015; Yue *et al*., 2015). There are also reports on the study of biological activities of lanthanide salen/salen-type complexes(Feng *et al.*, 2017; Taha *et al*., 2011). Lanthanides have an interesting but not well-understood biological role in living organisms as trace elements (Oruma *et al.*, 2014). Reports(Kostova *et al.*, 2005*;* Manolov *et al*., 1999; Kostova *et al*., 2004; Kostova *et al*., 2005) have shown that lanthanide(III) complexes of coumarins exhibit potent cytotoxic and cytostatic activities. Lanthanide-

salophen complexes have been reported to exhibit physiological activities for several pathological conditions including ovarian cancer (DallaCort*et al.*, 2010). Recently,Taha *et al*.,(Taha *et al*., 2011) reported that Nd, Dy, Sm, Pr, Gd, Tb and Er complexes with bis-(salicylaldehyde)-1,3-propylenediimine Schiff base ligand possess high antibacterial activity against *Shigelladysenteriae, Pseudomonas aeruginosa* and *Proteus vulgaris* (Gram-negative bacteria).

In view of the noted biological properties of s-triazines and lanthanide(III) complexes, we synthesized and characterized 2,4,6-tris(4-carboxyphenylimino-4^1-formylphenoxy)-1,3,5-triazine (**H_3CT)** and its trinuclear Dy(III) and Er(III) salen capped complexes. Their*in vitro* antimicrobial, *in vivo* antimalarial activities and acute toxicity, were investigated. The experimental work was supplemented with the density functional theory method and molecular docking.

2.0 Materials and methods

2.1 Materials and measurements

The chemicals used were of analytical reagent grade, purchased from Zayo–Sigma and were used as supplied without further purification. Fischer Jones melting point apparatus was used for the determination of melting point and values obtained were uncorrected. A 10^{-4}mol/L solution of the complexes in methanol at room temperature was used for the determination of molar conductance using WTW-LF 90 conductivity meter. Electronic spectra (in DMSO) were recorded on UV-Vis 1800 SHIMADZU spectrophotometer. A Perkin–Elmer (Waltham, Massachusetts, USA) 100 series version 10.03.08 FTIR spectrophotometer was employed for infrared spectra of the compounds. The ^{1}H and ^{13}C NMR spectra of the compounds were recorded on a Bruker (Billerica, Massachusetts, USA) DPX 300 spectrometer in DMSO- d_6 at 300.13MHz and 75.47MHz respectively. LECO – CHN – 932analyzer was used for elemental analysis for C, H and N.

2.2 Synthesis of 2, 4, 6-tris (p-formylphenoxy)-1, 3, 5-triazine (2)

The method reported by Tahmassebi and Sasaki (Tahmassebi and Sasaki, 1994)was modified and adopted. *P*–hydroxybenzaldehyde (3.20 g, 0.026 mol) and 2,4,6-trichloro-1,3,5-triazine(**1**) (1.20g, 0.0065 mol) were added to a suspension of Na_2CO_3 (20 g) in 50 mL of benzene as shown in Scheme 1. The mixture was refluxed with stirring at 70 °C for 7 h and left stirring overnight. During this time, the colour of the Na_2CO_3 changed from white to brown. The mixture was filtered and the residue was washed with hot ethyl ethanoate (20 mL) twice and both filtrates were mixed. The filtrate was divided into two and one part was placed in a separating funnel and 10 mL of 10 % Na_2CO_3 (2 g of Na_2CO_3 made up to 20 mL) was poured into it, shake properly and allowed to stand. Two layers were formed: a pink aqueous layer (below) and a golden organic layer (on top). The aqueous layer was discarded and the organic layer was further extracted with 10 mL of 10 % Na_2CO_3. The filtrate was extracted with water once. The organic layer was dried over anhydrous Na_2SO_4 and then concentrated. The white fluffy precipitate was recrystallized from ethyl acetate (20 mL), air-dried and stored over $CaCl_2$. This gave 2, 4, 6-tris (*p*-formylphenoxy)-1, 3, 5-triazine (**2**).

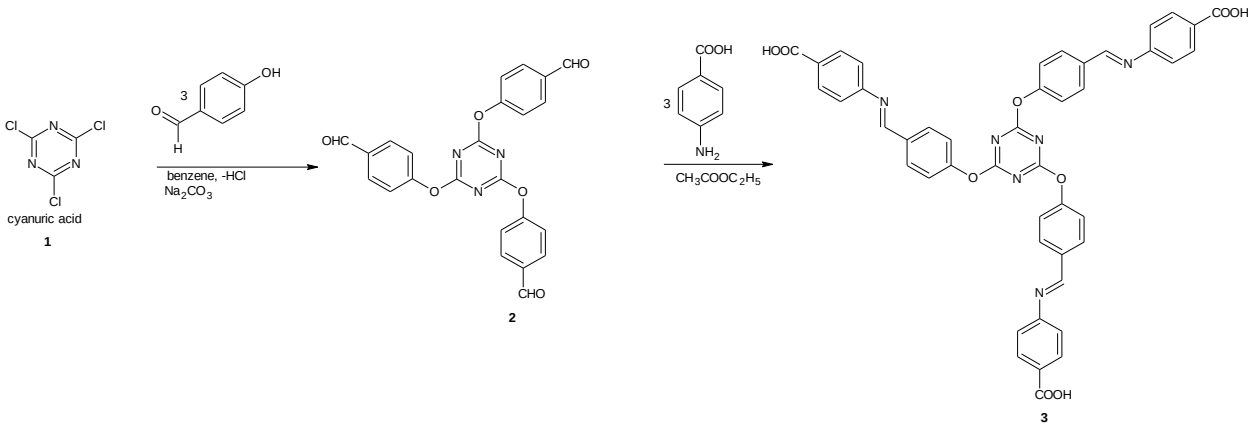

Scheme 1: Synthesis of 2, 4, 6-tris (4-carboxyphenylimino-4[1]-formylphenoxy)-1, 3, 5-triazine (H_3CT) (3)

2.3 Synthesis of 2, 4, 6-tris (4-carboxyphenylimino-4[1]-formylphenoxy)-1, 3, 5-triazine(H_3CT) (3)

The method reported by Koc and Ucan (Koc and Ucan, 2007) was adopted. Solid K_2CO_3 (1.55 g, 25 % excess of 0.009 mol) was added to a solution of 4-aminobenzoic acid (0.003 mol, 0.51 g) in 20 mL of ethyl ethanoate with stirring. The suspension of compound (**2**) (0.44 g, 0.001mol) in 10 mL of ethyl ethanoate was added dropwise with stirring. This is displayed in Scheme 1. The mixture was then boiled under reflux for 24 h. The reaction solution was left stirring overnight. Water was added to the mixture and filtered to remove some insoluble impurities. HCl (0.5 N) was added to the solution until the pH of 5 was attained and the mixture was filtered. The filtrate was evaporated slowly over the day and yellow crystals were precipitated. The yellow crystals (**3**) obtained were recrystallized from absolute ethanol, dried and stored in a desiccator over $CaCl_2$. Yield 0.47g (58.75 %), mp 282 °C; UV (DMSO) λ_{max}nm (ε): 230 (6.93 x10^3), 283 (5.85 x10^3); IR(KBr): 3239(O-H), 1594, 1546 (C=N), 1480 (C-C), 1394, 1384, 1367 (COO-), 1111 (C-N); ^{1}H NMR (DMSO- d_6, 300.13MHz): δ = 8.30(1H, s), 6.12 – 6.55(4H, d), 7.47 – 7.63(4H, d), 3.34(H_2O), 2.50(DMSO); ^{13}C NMR (DMSO- d_6, 75.47MHz): δ = 130.65(Ar – C), 112.54(Ar – C), 39.91(DMSO); Anal. Calcd for $C_{45}H_{30}N_6O_9$(798):C, 67.67; H, 3.76; N, 10.53 Found: C, 67.50; H, 3.60; N, 10.70. The UV, IR, ^{1}H NMR and ^{13}C NMR spectra are presented in supplementary materials S6, S14, S17 and S20 respectively.

2.3 Synthesis of the trinuclearLn(III)Salen Capped Complex of H_3CT

This involves the synthesis of:

1. salenH_2
2. Dy(III) and Er(III) salen complex
3. Dy(III) and Er(III) ligand complex, ([{Dy/Er(salen)}$_2$O])
4. Dy(III) and Er(III) Salen Capped Complex of H_3CT, $([\{Dy/Er(salen)\}_3(H_3CT)]^{3+} . 3H_2O)$

2.3.1 Synthesis of salenH_2

SalenH_2 was synthesized by modifying the method reported by Sathe *et al*. (Sathe *et al.*, 2013). To a solution of ethylenediamine(3.35 mL, 0.05mol) in methanol (50 mL) was added salicylaldehyde (10.47 mL, 0.1mol) in a round bottom flask. A yellow crystalline solid product was formed immediately. The yellow product was filtered and recrystallized from absolute ethanol(50 mL) at 80 °C to obtain yellow crystals. Yield = 11.14 g (83 %); mp of 109–110°C; UV(DMSO) λ_{max} nm (ε):316 (1.91 × 10^4), 404 (0.41 × 10^4);IR (KBr): 3441 (br)((O-H) Phenolic), 1608 (s) (C═N),1287(m) (C–O),751 (m)(C–H) cm^{-1};Anal. calcd for$C_{16}H_{16}O_2N_2$ (268): C, 71.64; H, 5.97; N, 10.45. Found: C, 71.60; H, 6.00; N, 10.30. The

UV and IR spectra are presented in supplementary materials S1 and S9.

2.3.2(a) Synthesis of Dy(III) salen complex

The method reported by Gembickỳ *et al.* (Gembicky *et al*., 2000) was modified and adopted for the synthesis of salen complexes. To a hot methanolic solution (40 mL) of salenH_2 (1.34g, 0.005mol), a hot methanolic solution (50 mL) of $Dy(NO_3)_3$. $5H_2O$ (2.2 g, 0.005mol) was added. A yellow precipitate was formed. The mixture was stirred at 50 °C for 30 min., and then triethylamine (0.02mol, 4 mL) was added. The yellow precipitate dissolved and a clear solution was obtained. The resulting clear solution was stirred at 50 °C for 2h and after cooling a milk coloured precipitate was formed. The precipitate was washed with methanol and diethyl ether and dried over $CaCl_2$. Yield = 2.35 g (72.31 %); mp of 298[a] °C(a = decomposition temperature)°C; UV (DMSO) λ_{max}nm (ε): 225 (5.44 x10^4), 349 (0.91 x10^4); IR(KBr): 3436 (O-H), 1631 (C=N), 1198 (C-O), 1458, 1041,894,1388 (NO_3^-), 755 (C-H), 586 (Ln-O), 400 (Ln-N); ^{1}H NMR spectrum could not be taken due to their paramagnetic character; Anal. Calcd for $[Dy(L)(NO_3)_2(H_2O)_2]NO_3$ (650.50): C, 29.52; H, 2.77; N, 10.76. Found: C, 29.30; H, 2.90; N, 10.64. L = salen. The UV and IR spectra are presented in supplementary materials S2 and S10.

2.3.2(b) Synthesis of Er(III) salen complex

To a hot methanolic solution (40 mL) of salenH_2 (1.34g, 0.005mol), a hot methanolic solution (50 mL) of $Er(NO_3)_3$. $5H_2O$ (2.23 g, 0.005mol) was added. The mixture was stirred at 50 °C for 30 min and a yellow product formed, then triethylamine (0.02mol, 4 mL) was added. On adding triethylamine, the yellow precipitate dissolved. The resulting clear solution was stirred at 50 °C for 2h and after cooling a milk coloured precipitate was formed. The precipitate was washed with methanol and diethyl ether and dried over $CaCl_2$. Yield = 2.18 g (66.56 %); mp of 350[a] °C(a = decomposition temperature)°C; UV (DMSO) λ_{max}nm (ε): 350 (3.49 x10^4); IR(KBr): 3434 (O-H), 1631 (C=N), 1193 (C-O), 1451, 1041,884,1390 (NO_3^-), 755 (C-H), 597 (Ln-O), 417 (Ln-N); ^{1}H NMR spectrum could not be taken due to their paramagnetic character; Anal. Calcd for $[Er(L)(NO_3)_2(H_2O)_2]NO_3$ - (655.26): C, 29.30; H, 2.75; N, 10.68. Found: C, 29.40; H, 2.80; N, 10.78.The UV and IR spectra are presented in supplementary materials S3 and S11.

2.3.3.(a) Synthesis of Dy(III) ligand complex, [{Dy(salen)}$_2$O]

The ligand complexes were prepared by modifying the method reported by Kopel *et al.* (1998) and Uysal *et al*.(2010; 2009).A solution of Dy(III) Salen complex (0.50 g, 10^{-3}mol) in absolute ethanol (20 mL) was stirred at 50 °C for 15 min. Excess concentrated ammonia solution (1 mL at a time) was added and stirred. The pH of the solution was monitored with the aid of a pH meter until the pH of 12. A milk coloured precipitate was formed, filtered and dried over $CaCl_2$.

Yield = 0.48 g (71.64 %); mp of 275[a] °C(a = decomposition temperature)°C; UV (DMSO) λ_{max}nm (ε): 263 (12.39 x10^3), 339 (4.48 x10^3); IR(KBr): 1627 (C=N), 1546 (C=C), 1272 (C-O), 887, 755 (C-H), 600 (Ln-O-Ln), 574 (Ln-O); ^{1}H NMR spectrum could not be taken due to their paramagnetic character; Anal. Calcd for [{Dy(salen)}$_2$O] (873): C, 43.99; H, 3.21; N, 6.41. Found: C, 44.10; H, 3.25; N, 6.54. The UV and IR spectra are presented in supplementary materials S4 and S12.

2.3.3.(b) Synthesis of Er(III) ligand complex, [{Er(salen)}$_2$O]

A solution of Er(III) Salen complex (0.50 g, 10^{-3}mol) in absolute ethanol (20 mL) was stirred at 50 °C for 15 min. Excess concentrated ammonia solution (1 mL at a time) was added and stirred. The pH of the solution was monitored with the aid of a pH meter until the pH of 12. A pale yellow precipitate was formed, filtered and dried over $CaCl_2$. Yield = 0.45 g (67.16 %); mp of 275[a] °C(a = decomposition temperature)°C; UV (DMSO)

λ_{max}nm (ε): 264 (5.42 x10^3), 348 (1.41 x10^3); IR(KBr): 1625 (C=N), 1544 (C=C), 1285 (C-O), 906, 753 (C-H), 598 (Ln-O-Ln), 574 (Ln-O), 438 (Ln-N); ^{1}H NMR spectrum could not be taken due to their paramagnetic character; Anal. Calcd for [{Er(salen)}$_2$O] (882.52): C, 43.51; H, 3.17; N, 6.35. Found: C, 43.70; H, 3.20; N, 6.57. The UV and IR spectra are presented in supplementary materials S5and S13.

2.3.4. Syntheses of the tripodal- trinuclear Dy(IIII) and Er(III) Salen Capped Complexes of H_3CT, ($[\{Dy/Er(salen)\}_3(H_3CT)]^{3+}.3H_2O$)

The trinuclear complexes were prepared by the reaction of two moles of the ligand**(H_3CT)** separately with three moles of [{Dy/Er(salen)}$_2$O] (ligand complexes(LC))as shown in Scheme 2.

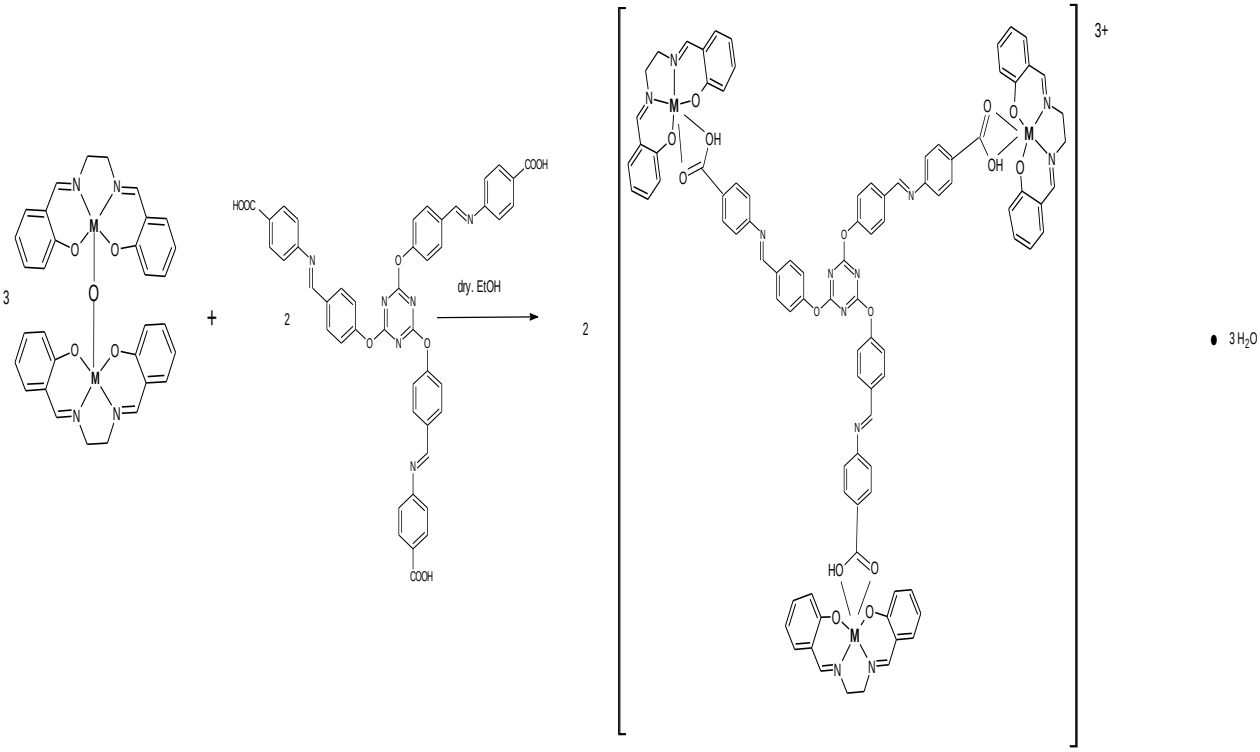

Scheme 2: Synthesis of $[\{Dy/Er(salen)\}_3(H_3CT)]^{3+}.3H_2O$

2.3.4.(a) Synthesis of $[\{Dy(salen)\}_3(H_3CT)]^{3+}.3H_2O$

[{Dy(salen)}$_2$O] (0.54 g, 0.00062 mol) was suspended in hot absolute ethanol (25 mL) and a solution of H_3CT (**3**) (0.33 g, 0.00041 mol) in absolute ethanol was added while stirring. The reaction mixture was heated at reflux for 4 h. The cream coloured solid formed was dried over $CaCl_2$. Yield 0.47g (53.41 %), mp 332[a](a = decomposition temperature)°C; UV (DMSO) λ_{max}nm (ε): 346 (4.38 x10^3); IR(KBr): 3024 (C-Har), 1625, 1593, 1538 (C=N), 1467, 1448, 1432 (C-C), 1390, 1340, 1332 (COO-), 1144, 1121(C-N), 593, 569 (Ln-O), 456, 432 (Ln-N); ^{1}H NMR (DMSO-d_6, 300.13MHz): δ = 12.98(1H, s), 8.83 (1H, s), 6.32- 6.95(4H,d), 4.12(4H, s)2.93(H2O), 2.49(DMSO); ^{13}C NMR spectrum could not be taken due to their paramagnetic character; Anal. Calcd for $C_{93}H_{78}O_{18}N_{12}Dy_3$(2,137.50):C, 52.21; H, 3.65; N, 7.86. Found: C, 52.43; H, 3.59; N, 7.94. The UV, IR, ^{1}H NMR and ^{13}C NMR spectra are

presented in supplementary materials S7, S15, S18 and S21 respectively.

23.4.(b) Synthesis of [{Er(salen)}$_3$(H$_3$CT)]$^{3+}$. 3H$_2$O

[{Er(salen)}$_2$O] (0.55 g, 0.00062 mol) was suspended in hot absolute ethanol (25 mL) and a solution of H_3CT (**3**) (0.33 g, 0.00041 mol) in absolute ethanol was added while stirring. The reaction mixture was heated at reflux for 4 h. The milky solid formed was dried over $CaCl_2$. Yield 0.47g (51.69 %), mp 335^a(a = decomposition temperature)°C; UV (DMSO) λ_{max}nm (ε): 355 (10.30 x10^3); IR(KBr): 1626, 1595, 1539 (C=N), 1468, 1448, 1432 (C-C), 1391, 1339 (COO-), 1147(C-N), 595, 572 (Ln-O), 456, 438 (Ln-N); ^{1}H NMR (DMSO-d$_6$, 300.13MHz): δ = 11.35(1H, s), 8.35(1H, s), 3.40(H2O), 2.50(DMSO); ^{13}C NMR spectrum could not be taken due to their paramagnetic character; Anal. Calcd for $C_{93}H_{78}O_{18}N_{12}Er_3$(2,151.78):C, 51.86; H, 3.62; N, 7.81. Found: C, 51.94; H, 3.76; N, 7.99. The UV, IR, ^{1}H NMR and ^{13}C NMR spectra are presented in supplementary materials S8, S16, S19 and S22 respectively.

2.4 In vitro antimicrobial activity

The tripodal ligand and its trinuclear complexes were tested *in vitro* for their antimicrobial activities against American Type Culture Collection (ATCC) bacteria strain obtained from Rockville, MD, USA, by the Department of Microbiology, University of Nigeria, Nsukka while the fungi strains were isolated under clinical conditions. The typed bacteria culture consists of Gram-positive bacteria: *Staphylococcus aureus* (ATCC 6538P) and *Bacillus cereus* (ATCC 14579); Gram-negative bacteria: *Escherichia coli* (ATCC 6749) and *Pseudomonas aeruginosa* (ATCC 9027). The fungi strains used were *Candida albicans* and *Aspergillus niger*. The fungal strains were tested on Sabourand Dextrose Agar(SDA) and cultured in Sabourand Dextrose Liquid medium at 25 °C for 24 h while the bacteria strains were tested for sterility on nutrient agar and then grown in nutrient broth at 37 °C for 24 h. The overnight cultures were subsequently diluted and suspensions were made in normal saline and adjusted to 0.5 McFarland standards (Cheesbrough 2006).

2.5 Antimicrobial assay

The agar cup diffusion technique (Alli*et al.*, 2011) was employed in the determination of the antimicrobial activities of all the synthesized compounds. The nutrient agar and SDA plates were inoculated with 0.1 mL broth culture of the test bacteria or fungi. Using a sterile cork borer, wells (5 mm in diameter and 2.5 mm deep) were bored into the inoculated agar. Fresh stock solutions (1000 µg/mL) of the synthesized compounds were prepared in DMSO. The stock solution was further diluted with sterilized distilled water to 12.5, 25, and 50 µg/mL for antimicrobial evaluation. The wells were filled with 100 µL of the test compounds using a sterile micropipette. Standard antibiotics namely: Ciprofloxacin, tetracycline, gentamycin and fluconazole served as positive control while sterile DMSO served as a negative control. Subsequently, 12.5, 6.25, and 3.125 µg/mL of each positive control were prepared in DMSO. The bacteria plates were incubated at 37 ^{o}C for 24 h while fungal plates were incubated at 25 ^{o}C for 24 h. Inhibition zone diameter (IZD) around each well was measured in millimeters and recorded. The graph of IZD^2 against the log of concentration was plotted for each plate containing a specific compound and a microorganism. The anti-log of the intercept on the *x*-axis is the MIC.

2.6 Determination of acute toxicity (LD$_{50}$)

Ethical approval: "All experiments involving the use of mice were conducted in compliance with NIH guidelines for care and use of animals (Council 2010)". [{Dy(salen)}$_3$(H$_3$CT)]$^{3+}$. 3H$_2$Owas used for the test because it showed higher sensitivity against the tested micro-organisms. The oral acute toxicity of the ethanolic solutions of the samples wasestimated in albino mice (100-250 g) by upper level lethal dose (LD_{50}) described

by Lorke'smethod (Lorke, 1983). Four mice of both sexes were employed and an acclimatization period of 24 h was allowed. The samples were weighed and dissolved in 3 % ethanol. The ethanolic solutions of the samples were administered orally at doses of 1000, 1600, 2900 and 5000 mg/kg. The animals were monitored for 24 h and the number of deaths per group was recorded. Then, the mice were observed continuously for one hour after treatment, intermittently for three hours and thereafter for 24 h. The mice were observed for gross behavioral changes such as feeding, hair erection, lacrimation, mortality and other signs of toxicity manifestation. The mice were given access to food and clean water during the study.

2.7 In vivo studies

The *in vivo* antimalarial assay was done based on a 4-day suppressive test using mice. The evaluation of the antimalarial activity against the methanolic solutions of the samples and Artesunate sensitive *Plasmodium berghei* (NK 65) was carried out according to a standard protocol of Peter's 4-day suppressive test (Peters, 1975). Each of the 12 healthy experimental mice was inoculatedintraperitoneally on the first day (Day 1). The infected mice were weighed and randomly divided into four groups of three mice each and four hours post-inoculation were treated orally thereafter 24, 48 and 72 h post inoculation. For groups 1 and 2, 25 mg of sample/kg of mouse and 50 mg of sample/kg of mouse were administered orally for four consecutive days. For group 3, 5 mg of Artesunate/kg of the mouse was administered while group 4 was given 5 mL of distilled water/kg of the mouse for four consecutive days. A blood smear was taken on day 5. On day 4 post-inoculation, one drop of blood was taken from the tail of each experimental mouse and smeared on a microscope slide to make a thin film (Saidu *et al*., 2000). The thin films were fixed with methanol, stained with 10 % Giemsa solution at pH 7.2 for 10 mins and examined microscopically. Parasitemia level was determined by counting the number of parasitized erythrocytes out of 100 erythrocytes per field in 4 random fields under a light microscope at magnification (×100) while average percentage parasitemia suppression was determined by comparing the parasitemia in the control group with the treated group.

Average percentage suppression = $pc - \frac{pt}{pc} \times 100$ (Ukwe *et al.*, 2010)

where pc is the average parasitemia in the control group and pt average parasitemia in the treated group.

2.8 Computational method

Geometric optimization for $C_{45}H_{30}N_6O_9$, H_3CTwas performed using Becke 3 Lee Yang par (Becke, 1992), (B3LYP)/6-31+G(d,p). The IR spectrum was studied by performing a frequency calculation and the electronic (UV) calculation was determined using time-dependent density functional theory (TDDFT) (Runge and Gross, 1984; Suendo and Viridi, 2011). The energy of the highest molecular orbital (HOMO) and that of the lowest molecular orbital (LUMO) (Chen *et al*., 2009; Rauf *et al*., 2015; Chioma *et al*., 2018) of the ligand was estimated using 6-31+G(d,p).

Molecular docking was performed to determine the binding energies on the inhibition potentials of *Staphylococcus aureus*. The 3D PDB structures were retrieved from the Protein data bank (PDB) for *Staphylococcus aureus* access code: 3k4q (Oakley, 2010), (resolution 2.2 Å). The grid box size for the possible binding site was determined using AutoDock 1.5.4. tools (Sanner 1999)and the dimension was X= 44, Y= 42, Z= 40 with 1.00 Å as the grid spacing. Gasteiger (Yang *et al.*, 2013)charges were added using the AutoDock Tools graphical user interface provided by MGL Tools (Morris *et al.*, 2009). The binding site for the ligand was obtained using the Lamarckian genetic algorithm method. The ligand was optimized using Gaussian 09 (Frisch *et al.*, 2009), to obtain minimum structures.

3.0 Results and Discussion

The analytical data of H_3CT and its trinuclear complexes are in good agreement with the proposed molecular formula as shown in Table 1. Molar conductivity measurements in methanol at room temperature show that the trinuclear complexes are 1:1 electrolytes while the ligand is neutral(Ali *et al*., 2013).

Table 1: Elemental and physical data of2,4,6 - tris(4-carboxyphenylimino-4[1]-formylphenoxy) -1,3,5-triazine (H_3CT) and its Dy/Er(III) complexes

Compound	Colour	Λ_m ($\Omega^{-1}cm^2mol^{-1}$)	Yield g (%)	M.p. (°C)	Elemental analysis % calcd. and found					
					C		H		N	
					Calcd.	Found	Calcd.	Found	Calcd.	Found
$C_{45}H_{30}N_6O_9$ (H_3CT)	Yellow	-	0.47 (58.75)	282	67.67	67.50	3.76	3.60	10.53	10.70
$[\{Dy(salen)\}_3(H_3CT)]^{3+}.3H_2O$	Creamy	87	0.47 (53.41)	332[a]	52.21	52.43	3.65	3.59	7.86	7.94
$[\{Er(salen)\}_3(H_3CT)]^{3+}.3H_2O$	Milky	120	0.46 (51.69)	335[a]	51.86	51.94	3.62	3.76	7.81	7.99

[a] = decomposition temperature, Standard 1:1 electrolyte in Methanol = 80 – 122 ohm^{-1}cm^{2}mol^{-1}

3.1 Computational Analysis

3.1.1 DFT Analysis

The fully optimized geometries of H_3CT is presented in Fig. 1. This was done to obtain a global minimum structure.

The highest occupied molecular orbital (HOMO) and lowest unoccupied molecular orbital (LUMO) (Fig. 2) are presented in the form of frontier molecular orbitals (FMO) (Rauf *et al*., 2015; Dumont, 2013). The electron donating ability of a complex is related to the E_{HOMO} and in general, the higher the E_{HOMO} energy (less negative), the more the ability to donate electrons (Ibeji*et al*., 2015; Ekennia *et al.*, 2017). The ligand showed a low ΔE (band) gap (E_{LUMO} - E_{HOMO}) of 2.11 eV suggesting high reactivity. The bandgap (or the π–π* electron transition) was estimated as the difference between the HOMO and LUMO orbital energies (Table S4). The negative value of HOMO energy is referred to as IP (Ibeji *et al.*, 2015; Salzner 2008; Ibeji *et al.*, 2018), whereas the negative values of LUMO is called the EA (Rauf *et al*., 2015; Ekennia *et al*., 2018).To further elucidate on the reactivity of ligand, the electronegativity (μ), chemical hardness (η) and softness (S) was determined according to the equations:

Chemical hardness, η (1)

Global softness (2)

Electronegativity $\mu \approx -\chi = -$ (3)

where I and A are the ionization potential and electron affinity, $I = -E_{HOMO}$ and $A = -E_{LUMO}$, respectively.

As shown in Table S4, the compound studied is The simulated IR spectrum of H_3CT is in good agreement with the experimentally observed. H_3CT shows a very broad peak at 3241 cm^{-1} assigned to the carboxylic OH group vibration. The IR spectrum ofH_3CT showed two strong peaks for C=N(a) and C=N(b) at 1511 and 1525 cm^{-1} respectively.

The predicted absorption UV spectra were also carried out on the ligand using TDDF based on the optimized geometry obtained by B3LYP/6-31+G(d,p). The results obtained indicated that the most intense peak is shown at 286 nm with an oscillator strength of 1.21described as an allowed π- π* transition corresponding to HOMO—LUMO transition and a molecular contribution (Olanrewaju *et al*., 2018)of 53.5%. This agrees with the obtained experimental data. Another peak was also

observed at 300 nm corresponding to HOMO—LUMO-1 transition with a molecular contribution of 61.8%. This is described as a forbidden transition since the oscillator strength is 0.1(Olanrewaju *et al*., 2018). As seen in Fig. 2, more electron density is delocalized in the HOMO orbital compared to the LUMO which is the lowest unoccupied orbital.

3.1.2 Molecular docking

Molecular docking studies were performed to gain further insight into the inhibition potentials of the ligand, which will further help in projecting the binding abilities of the metal complexes. Docking result showed inhibition potentials with the ligand. This is evident in the hydrogen bond interactions around the active amino acid residues (Fig. 3). A similar protocol was performed by Bharatham*et al*(Bharatham *et al*., 2008).

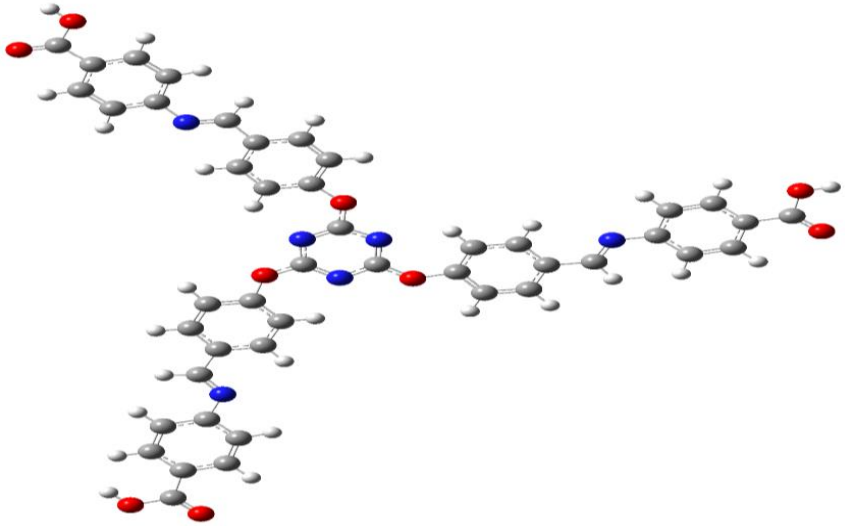

Fig.1: Optimized structure of H_3CT obtained at B3LYP)/6-31+G(d,p) (red = oxygen atom; blue = nitrogen atom; white = hydrogen atom; and grey = carbon atom)

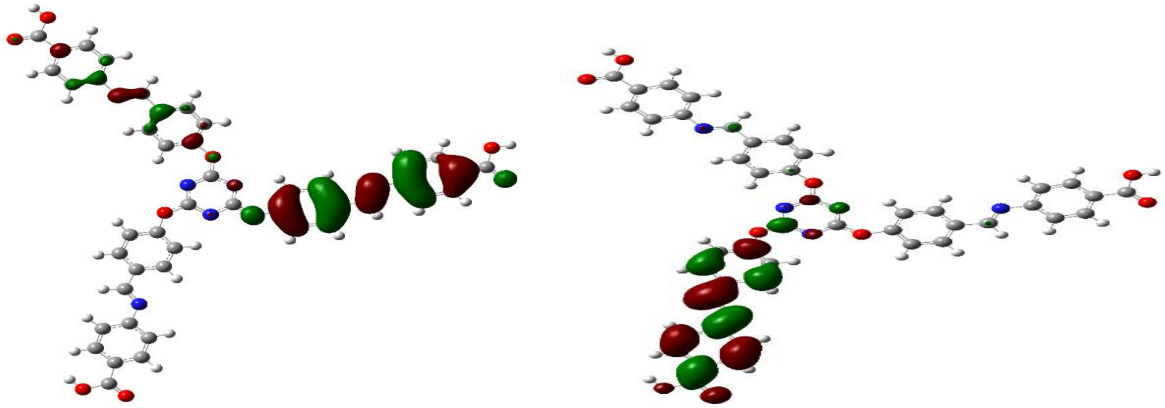

HOMO-H_3CT **LUMO-H_3CT**

(a) **(b)**

Fig.2: FMO orbital diagram showing the distribution of electron delocalization obtained byB3LYP/6-31+G(d,p)

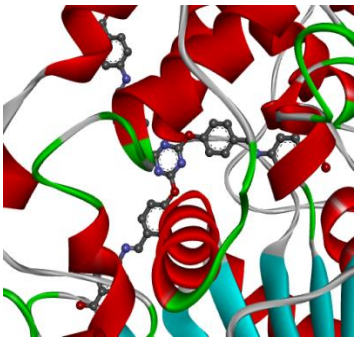

(a)

(b)

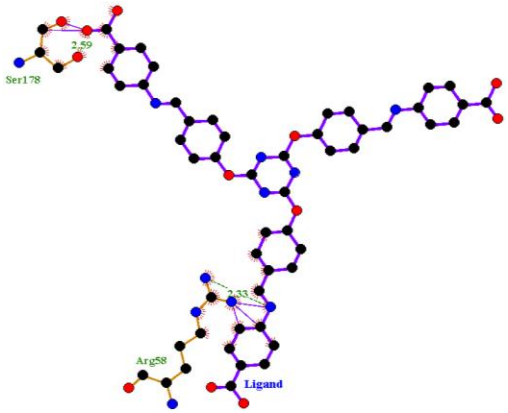

Fig. 3: 3D structure of (a) complex and (b) the interacting residues (with hydrogen bonding and hydrophobic) around the binding pocket of H_3CT complexed with *Staphylococcus aureus*

From the docking result (Table 2), the binding mode analysis of the ligand with some amino acid residues provided important information for proposing the catalytic mechanism.

Table 2: Calculated binding energy, core amino acid residue and hydrogen bond distance between residues and H_3CT from molecular docking

Enzymes	Binding energy (kcal/mol)	Residues	Atoms of the residues	Distance (Å)
Staphylococcus aureus	-5.45	SER, ARG	O, N, C	2.59, 2.33

3.2 Electronic spectra

The UV/Vis absorption spectra of H_3CT and its complexes (10^{-5} M) were carried out in DMSO at room temperature in the range 200 – 800 nm. The spectral values of the absorption wavelength and the corresponding molar absorptivities (ε) are given in Table 3. The absorption spectra are displayed in supplementary materials. The absorption spectrum of H_3CT shows two peaks at 230 and 283 nm assigned to π–π* transitions of the conjugated phenyl ring. The absorption spectra of the complexes show only one peak. This peak is assigned to charge transfer (LMCT) from the ligand, H_3CT, to the lanthanide ions.A similar observation has been made in the literature for Er(III) ions (Taha *et al*., 2011; Fei *et al.,* 2016).

The changes in the values of ε indicate the formation of the Ln(III) complexes. There are no peaks due to f transition, since in lanthanides f –f transitions are Larporte-forbidden and very weak, they do not contribute much to the spectra of their complexes (Taha *et al*., 2011; Cristóvão and Hnatejko, 2015; Görller-Walrandand Binnemans, 1998).

3.3 IR Spectra

The IR spectrum of the tripodal ligand, $H_3CT$and its trinuclear complexes are displayed in Table 4.H_3CT displayed a very broad band centered at 3239 cm^{-1}. This band was assigned to the carboxylic OH group vibration(Kocand Ucan, 2007). However, in the complexes, this band did not disappear but shifted to a higher wavenumber in the range 3239 –3260 cm^{-1}suggesting that the carboxylic

OH was not deprotonated before coordination to the Ln metal. The IR spectrum of H_3CT showed two strong bands for C=N(a) and C=N(b) at 1546 and 1594 cm^{-1} respectively. However, in the complexes, three bands were observed: C=N(a) bands at 1593 – 1595 cm^{-1}, C=N(b) bands at 1623 –1626 cm^{-1} and C=N(c) bands at 1530 –1539 cm^{-1} respectively. Similar observation has been made in literature (Uysal and Koç, 2016; Uysal and Uçan, 2009 (a); Uysal*et al.*, 2012). The C=N(a) and C=N(b) stretching vibration in the complexes shifted to higher wavenumber in comparison to the same transition in the ligand indicating delocalization of the double bond of the tripodal Schiff base on coordinating with the ligand complexes. While the C =N(c) band, which was absent in the tripodal Schiff base ligand but present in the complexes confirms that the ligand complexes were capped to the tripod. Similar observation has been made in literature (Uysal and Uçan, 2009 (a); Uysal and Uçan, 2009 (b)).The vibration due to the COO^- group, was observed between 1332 –1394 cm^{-1} in the compounds. This band shifted to lower frequencies in the complexes suggesting the involvement of the COOH group in coordination with the Ln ions; (Uysal and Uçan, 2009 (a); Uysal *et al.*, 2012). Bands at 569 – 595 and 432 – 456 cm^{-1} range are attributed to Ln –O and Ln –N stretch in the complexes and they confirm the binding mode (Taha *et al.*, 2011;Lekha *et al*., 2014).

Table 3: Electronic absorption data of 2,4,6-tris(4-carboxyphenylimino-4[1]-formyl phenoxy) -1,3,5-triazine (H_3CT) and its Dy/Er(III) complexes

Compound	λ_{max}		$\varepsilon\times10^3$ ($mol^{-1}dm^3cm^{-1}$)	Band assignment
	Nm	cm^{-1}		
H_3CT	230	43478	6.93	π–π*
	283	35336	5.85	π–π*
$[\{Dy(salen)\}_3(H_3CT)]^{3+}.3H_2O$	346	28901	4.38	LMCT
$[\{Er(salen)\}_3(H_3CT)]^{3+}.3H_2O$	355	28169	10.30	LMCT

Table 4: IR band assignments (cm^{-1}) for 2,4,6 - tris(4-carboxyphenylimino-4[1]-formyl phenoxy) -1,3,5-triazine (H_3CT) and its Dy/Er(III) complexes

Compound	ν (O – H)	ν (C = N)	ν C –C	υ COO-	ν C – N	ν Ln –O	ν Ln –N
H_3CT	3239(br)	1546(s)a 1594(s)b	1480	1394(s) 1384(s) 1367(s)	1111	-	-
$[\{Dy(salen)\}_3(H_3CT)]^{3+}.3H_2O$	3260(br)	1593(s)a 1625(s)b 1538(s)c	1467(s) 1448(s) 1432(m)	1390(s) 1340(m) 1332(s)	1144(m) 1121(m)	593(s) 569(m)	456(s) 432(m)
$[\{Er(salen)\}_3(H_3CT)]^{3+}.3H_2O$	3250(br)	1595(s)a 1626(s)b 1539(s)c	1468(s) 1448(m) 1432(m)	1391(s) 1339(s)	1147	595(m) 572(m)	456(m) 438(m)

where ν (O – H) = from carboxylic acid. Where C = N(a)= from triazine ring, C = N(b) = from azomethine linkage, C = N(c) = from salen.

3.4 ^{1}H NMR Spectra

The ^{1}H NMR spectra of H_3CT and its Dy/Er(III) complexes were recorded in D_6-DMSO (Table 5). The ^{1}H NMR spectra of H_3CT did not show the signal due to carboxylic OH. However, this peak was observed in $[\{Dy(salen)\}_3(H_3CT)]^{3+}.3H_2O$ and $[\{Er(salen)\}_3(H3CT)]^{3+}.3H_2O$suggesting that the trinuclear complexes were formed without deprotonation of the carboxylic proton (Koc and Ucan, 2007). The signal due to azomethine proton was observed downfield as

3. 5 ^{13}C NMR Spectra

The ^{13}C NMR spectra of H_3CT and its Dy/Er(III) complexes are displayed in supplementary materials while the spectral data are presented in Table 6. The ^{13}C NMR spectrum of H_3CT shows only two signals due to phenyl carbons at 112.54 and 130.65 ppm. The spectra for the trinuclear complexes show only solvent peak probably due to the extent of paramagnetism of the Ln(III) ions(Karatas, and Ucan, 2014).

a singlet at 8.30 ppm in H_3CT (Mohanan *et al*., 2014; Kadhum, 2011) and in the complexes, it suffers a downfield shift by about 0.05 –0.53 ppm. This confirms the bonding mode as suggested by IR studies. The signal due to phenyl protons reflects the two different chemical environments of the protons. In H_3CT, protons on phenyl ring, position 1 and 2 were observed between 6.12 – 6.55 ppm while the protons occupying position 3 and 4 on the second phenyl ring (Fig. 4) were observed between 7.47 – 7.63 ppm (Tahmassebi and Sasaki, 1994). The spectra also reveal that the compounds contain water of hydration (Silverstein *et al*., 2014).

3.6 In vitro antimicrobial activity

The results of the *in vitro* antimicrobial screening carried out on the compounds are given in Table 7. Ciprofloxacin, tetracycline, gentamicin and fluconazole were used as positive control while sterile DMSO served as a negative control. The structures of these drugs are shown in the supplementary material (Figure S23). Ciprofloxacin ($C_{17}H_{18}FN_3O_3$) belongs to fluoroquinolones and inhibits bacteria growth by preventing deoxyribonucleic acid (DNA) synthesis before mitosis. Tetracycline ($C_{22}H_{24}N_2O_8$) inhibits the multiplication of bacteria by binding to a subunit of the ribosomes, thereby inhibiting protein and nucleic acid synthesis and consequent death of the bacterium (Obasi*et al.*, 2017; Wolters, 2009).

Gentamycin ($C_{21}H_{43}N_5O_7$) belongs to the class of aminoglycosides and acts by preventing protein synthesis, thereby inhibiting the synthesis of nucleic acids (DNA replication or RNA synthesis) and causes the death of the bacterium. Fluconazole is an antifungal drug ($C_{13}H_{12}F_2N_6O$) and belongs to synthetic triazoles. Fluconazole inhibited fungal cytochrome P –450, an enzyme responsible for fungal sterol synthesis, thereby causing fungal cell walls to weaken (Wolters 2009).

The results obtained (Table 7) show that the compounds inhibited the growth of *Bacillus cereus*, *Staphylococcus aureus*, *Pseudomonas aeruginosa*, *Escherichia coli*, *Candida albicans*,and*Aspergillus niger* with inhibition zone diameter (IZD) in the range of 2 – 11, 2 – 11, 2 – 12, 4 – 5, 7 – 19, 5 –10 mm respectively. This reflects that the compounds exhibit higher activity against fungi (*Candida albicans* and *Aspergillus niger*) relative to the bacteria strains used. Among the test bacteria, the compounds were most active against *Pseudomonas aeruginosa* and had the same activity against Gram positive bacteria (*Staphylococcus aureus* and *Bacillus cereus*). It was observed from the results(Table 7) that the activity of the trinuclear complex in most cases is higher than that of the tripodal ligands. The enhanced activity of the trinuclear complexes could be ascribed to the increased lipophilic nature of the complexes arising due to anion

coordination (Mohanan *et al*., 2006).The Ln – salen complexes act as Lewis acids. Thus, are potential receptors for anions that can donate lone pair of electrons to the Ln metal (DallaCort *et al.*, 2010). The cell walls and cell membranes of the micro-organisms contain majorly lipids and polysaccharides. The interaction of the Ln ions with these cellular compounds are because all these structures contain a variety of functional groups that can donate lone pair of electrons to the metal (Chakrabarti 1995). This enables the compounds to penetrate the cell wall and cell membrane of the micro-organisms and interfere with the normal cell processes.

The inhibition zone diameter (IZD in mm) of the controls is displayed in Table S1. From Table S1, the inhibition zone diameters (IZD) of the controls are higher than that of the compounds. The minimum inhibitory concentration (MIC) of the compounds and controls against *Bacillus cereus*, *Staphylococcus aureus, Pseudomonas aeruginosa, Escherichia coli, Candida albicans,* and *Aspergillus niger* are displayed in Table 8. From Table 8, the MIC of the compounds is found to be in the range 25 for *Bacillus cereus***,** 25 – 50 for *Staphylococcus aureus,* 25 – 50 for *Pseudomonas aeruginosa,* 50 for *Escherichia coli,* 25 – >50 for *Candida albicans*and25 –50 for *Aspergillus niger***.**

Table 5:^{1}H NMR data of 2,4,6 - tris(4-carboxyphenylimino-4^{1}-formyl phenoxy) -1,3,5-triazine (H_3CT) and its Dy/Er(III) complexes (ppm)

Compound	OH carboxylic	CH = N	$H_{aromatic}$	CH_2= CH_2	H_2O (hydration)	DMSO
H_3CT	-	8.30(1H,s)	6.12–6.55(4H,d) 7.47 – 7.63(4H,d)	-	3.34	2.50
[{Dy(salen)}$_3$(H_3CT)]$^{3+}$.3H_2O	12.98(1H,s)	8.83(1H,s)	6.32–6.95(4H,d)	4.12(4H,s)	2.93	2.49
[{Er(salen)}$_3$(H_3CT)]$^{3+}$.3H_2O	11.35(1H,s)	8.35(1H,s)	-	-	3.4	2.50

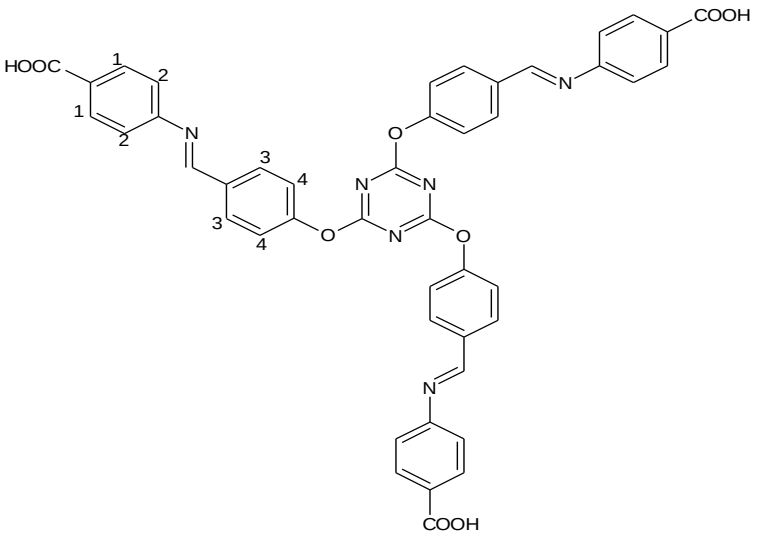

Fig. 4: Schematic drawing of H_3CT showing the positions of the protons

Table 6:[13] C NMR Spectral data of 2,4,6 - tris(4-carboxyphenylimino-4[1]-formyl phenoxy) - 1,3,5-triazine (H_3CT) and its Dy/Er(III) complexes (ppm)

Compound	Carboxylic carbon	Azomethine carbon	Carbons on triazine ring	Aromatic carbons	DMSO peak	Ethylene carbons
H_3CT	-	-	-	130.65, 112.54	39.91	-
$[\{Dy(salen)\}_3(H_3CT)]^{3+}.3H_2O$	-	-	-	-	39.88	-
$[\{Er(salen)\}_3(H_3CT)]^{3+}.3H_2O$	-	-	-	-	39.91	-

Table 7: Inhibition zone diameter (IZD in mm) of the compounds against typed strains (ATCC CULTURES) microorganisms

50 µg/Ml						
Compound	*B.c*(ATCC 14579)	*S.a*(ATCC 6538P)	*P.a*(ATCC 9027)	*E.c*(ATCC 6749)	*C.a*	*A.n*
H_3CT	11	2	3	4	-	9
$[\{Dy(salen)\}_3(H_3CT)]^{3+}.3H_2O$	10	11	12	5	13	10
$[\{Er(salen)\}_3(H_3CT)]^{3+}.3H_2O$	5	5	3	4	19	10
25 µg/Ml						
H_3CT	2	-	-	-	-	-
$[\{Dy(salen)\}_3(H_3CT)]^{3+}.3H_2O$	4	2	2	-	7	-
$[\{Er(salen)\}_3(H_3CT)]^{3+}.3H_2O$	2	2	-	-	-	5
12.5 µg/mL						
H_3CT	-	-	-	-	-	-
$[\{Dy(salen)\}_3(H_3CT)]^{3+}.3H_2O$	-	-	-	-	-	-
$[\{Er(salen)\}_3(H_3CT)]^{3+}.3H_2O$	-	-	-	-	-	-

Key:*B.c = Bacillus cereus, S.a = Staphylococcus aureus, P.a = Pseudomonas aeruginosa, E.c = Escherichia coli, C.a = Candida albicans.A.n = Aspergillus niger*, (-) = no zone of inhibition observed.

Table 8: Minimum inhibitory concentration (MIC) of the compounds and controls against test bacteria and fungi

MIC (µg/mL)						
Compound	*B.c*(ATCC 14579)	*S.a*(ATCC 6538P)	*P.a*(ATCC 9027)	*E.c*(ATCC 6749)	*C.a*	*A.n*
H_3CT	25	50	50	50	>50	50
$[\{Dy(salen)\}_3(H_3CT)]^{3+}.3H_2O$	25	25	25	50	25	50
$[\{Er(salen)\}_3(H_3CT)]^{3+}.3H_2O$	25	25	50	50	50	25
Controls						
T	1.90	1.80	0.63	2.15	2.10	0.58
F	6.25	6.25	6.25	2.80	0.64	0.74
CP	1.50	0.70	0.92	0.65	2.00	6.25
G	1.40	2.70	0.71	2.60	2.50	0.64

Legend: T = Tetracycline, F = Fluconazole, CP = Ciprofloxacin, G = Gentamycin

.

From Table 7, the MIC of the controls is found to be in the range 1.40 – 6.26 for *Bacillus cereus***,** 0.70 **–** 6.25 for *Staphylococcus aureus,* 0.63 – 6.25 for *Pseudomonas aeruginosa,* 0.65 – 2.80 for *Escherichia coli,* 0.64 – 2.50 for *Candida albicans* and 0.58-6.25 for *Aspergillus niger***.** From Table 7, it can also be seen that $[\{Dy(salen)\}_3(H_3CT)]^{3+}.3H_2O$ is most active against the test microorganisms relative to the compounds.

3.7 Acute toxicity

The acute toxicity test was recorded for $[\{Dy(salen)\}_3(H_3CT)]^{3+}.3H_2O$as shown in Table S2. $[\{Dy(salen)\}_3(H_3CT)]^{3+}.3H_2O$ was chosen because it shows higher sensitivity against the test micro-organisms. For mice administered with $[\{Dy(salen)\}_3(H_3CT)]^{3+}.$ $3H_2O$, no animal died within 24h after administration (Table S2). This implies that $[\{Dy(salen)\}_3(H_3CT)]^{3+}$ $.3H_2O$ is safe and have a wide range of effective dose (ED_{50}) (Alli*et al*., 2011).

3.8 In vivo anti-malarial studies

The suppressive antiplasmodic effect of methanolic solutions of the test samples on albino mice is displayed in Table S3 while Table 9 gives the percentage parasitemia inhibition. Artesunate is an antimalarial drug with molecular formula of $C_{19}H_{28}O_8$ It was used as standard because of the presence of –COOH group in both Artesunate and H_3CT. The structure is shown in Figure S2

Table 9: Percentage parasitemia inhibition

Drus/Dose (mg/kg)	% Parasitemia	%inhibition (PC)
$[\{Dy(salen)\}_3(H_3CT)]^{3+}.3H_2O$ 25	6.77 ± 1.76	78.59
$[\{Dy(salen)\}_3(H_3CT)]^{3+}.3H_2O$ 25	5.00 ± 0.58	84.02
Artesunate 5	4.00 ± 0.58	87.22
Dist. Water 5mL/kg	31.33 ± 3.38	00.00

The research work by Gopalakrishnana and Kumar has shown that artesunate induces DNA double-strand breaks in *P. falciparum* in a physiologically relevant dose- and time-dependent manner leading to parasite death (Gopalakrishnana and Kumar, 2015). It was observed from Table S3 that the effect of the samples on weight (Wt), PCV and Hb of the infected mice treated did not show an orderly pattern of dose dependent effect. However, the effect was significant comparing the negative control. $[\{Dy(salen)\}_3(H_3CT)]^{3+}.3H_2O$show a significant reduction with the effect of the sample on PCV dose dependently though in a negative manner. The effect of sample on Hb concentration shows the same effect as in PCV. Table 9 results show a general dose dependent significant parasitemia inhibition compared with the negative control with $[\{Dy(salen)\}_3(H_3CT)]^{3+}.3H_2O$having the highest inhibition of 84.02 % at 50 mg/kg close to the value (87.22 %) of the standard drug Artesunate 5 mg/kg. This implies that $[\{Dy(salen)\}_3(H_3CT)]^{3+}.3H_2O$ can be used as anti-malarial drugs after further tests.

4.0 Conclusion

A tripodal Schiff base ligand derived from 2,4,6-trichloro-1,3,5-triazine and its novel trinuclear Dy(III) and Er(III) Salen Capped Complexes were synthesized and characterized based on various physicochemical and spectral studies. The ligand was found to be tripodal and to coordinate to the ligand complexes via the carboxylic group. *In vitro* antimicrobial activity indicate that the trinuclear complexes are more active against the test micro-organisms relative to the ligand; with $[\{Dy(salen)\}_3(H_3CT)]^{3+}.3H_2O$ having the highest antimicrobial activity. Acute toxicity studies reveal that $[\{Dy(salen)\}_3(H_3CT)]^{3+}.3H_2O$ is safe and have

a wide range of effective dose (ED_{50}). *In vivo* antimalarial studies indicate that $[\{Dy(salen)\}_3(H_3CT)]^{3+}.3H_2O$ could serve as an effective anti-malarial agent since it has parasitemia inhibition of 84.02 % at 50 mg/kg close to the value (87.22 %) of the standard drug Artesunate 5 mg/kg. DFT calculations carried out enhanced more understanding of H_3CT at the molecular level. The molecular docking results revealed the binding mode of H_3CT complexed with *Staphylococcus aureus.*

5.0 Acknowledgments

The authors thank Dr. AnicetSiakamWendji, TechnischeUniversität, Dortmund, Germanyfor recording theNMR and IR spectra.We also acknowledge the support received from the African-German Network of Excellence in Science (AGNES), the Federal Ministry of Education and Research (BMBF) and the Alexander von Humboldt Foundation (AvH).

7.0 References

Afonso, C. A. M., Lourenco, N. M. T. & Rosatella A. D. A. (2006). Synthesis of 2,4,6-Tri-substituted-1,3,5-triazines. *Molecules* 11, pp. 81-102.

Ali, I, Wani, W. A. & Saleem, K. (2013). Empirical formulae to molecular structures of metal complexes by molar conductance. *Synthesis and Reactivity in Inorganic, Metal-Organic and Nano-Metal Chemistry* 43, pp. 1162-1170.

Alli Afonso, C. A. M., Lourenco, N. M. T. & Rosatella, A. D. A.(2006). Synthesis of 2,4,6-Tri-substituted-1,3,5-triazines. *Molecules*, 11, pp. 81-102.

Alli, A. I., Ehinmidu, J. O. & Ibrahim, Y. K. E. (2011). Preliminary phytochemical screening and antimicrobial activities of some medicinal plants used in Ebiraland. *Bajopas* 4, 1, pp. 10-16. ~~(1):10-16.~~

Arya, K., & Dandia, A. (2007). Synthesis and cytotoxic activity of trisubstituted-1,3,5-triazines. *Bioinorganc and Medicinal Chemistry Letters* ,17, 12, pp. 3298-3304.

Becke, A. D. (1992). Density-functional thermochemistry. I. The effect of the exchange-only gradient correction. *Journal of Chemical Physics,* 96, pp. 2155-2160.

Bespalov, V. G., Beliaeva, O. A., Panchenko, A. V., Stukov, A. N., Gershanovich, M. L., Murazov, I. G., Konkov, S. A., Kilmaeva, N. N., Krylova, I. M., Mironiuk, T. A. & Latipova, D. K. (2011). Antitumor activity of dioxadet compared with cispatin on ascetic ovarian tumor in rats. *Voprosy onkologii,* 57, 6, pp. 771- 774.

Bharatham, K., Bharatham, N., Park, K. H. & Lee, K. W. (2008). Binding mode analyses and harmacophore model development for sulfonamide chalcone derivatives, a new class of α-glucosidase inhibitors. *Journal of Molecular Graphics and Modelling,* 26, pp. 1202-1212.

Chandrakumar, K. & Pal, S. (2002). The Concept of Density Functional Theory Based Descriptors and its Relation with the Reactivity of Molecular Systems: A Semi-Quantitative Study. *International Journal of Molecular Sciences,* 3, 4, pp. 324-337.

Chakrabarti, P. (1993). Anion binding sites in protein structures. *Journal of Molecular Biology,* 234, pp. 463-482.

Cheesbrough, M. (2002). *District Laboratory Practice in Tropical Countries (low priced edition)*.Cambridge University Press, Edinburgh UK, pp. 393 - 394.

Chen, C., Chen, C., Yan, P., Hou, G. & Li, G. (2013). Structure and electrochemistry of salen cerium(IV) complexes tuned by multiform counter ions. *Inorganica Chimica Acta*, 405, pp. 182-187.

Chen, L., Liu, T. & Ma, C. A. (2009). Metal complexation and biodegradation of EDTA and S, S-EDDS: a density functional theory study. *The Journal of Physical Chemistry,* A 114, 1, pp. 443-454.

Chien, Y. –L., Chang, M. –W., Tsai, Y. –C., Lee, G. –H., Sheu, W. –S. & Yang, E. -C. (2015). New salen-type dysprosium(III)

double decker and triple decker complexes. *Polyhedron* 102, pp. 8-15.

Chioma, F., Ekennia, A. C., Ibeji, C. U., Okafor, S. N., Onwudiwe, D. C., Osowole, A. A., Ujam, O. T. (2018). Synthesis, characterization, antimicrobial activity and DFT studies of 2-(pyrimidin-2-ylamino) naphthalene-1, 4-dione and its Mn (II), Co (II), Ni (II) and Zn (II) Complexes. *Journal of Molecular Structure*, 1163, pp. 455-464.

Council, N. R. (2010). *Guide for the care and use of laboratory animals.* National Academies Press

Cristóvão, B. & Hnatejko, Z.(2015). Lanthanide (III) compounds with the N_2O_4-donor Schiff base -Synthesis, spectral, thermal, magnetic and luminescence properties. *Journal of Molecular Structure*, 1088, pp. 50 – 55.

DallaCort, A., De Bernardin, P., Forte, G. & Mihan, F. Y. (2010). Metal-salophen-based receptors for anions. *Chemical Society Reviews*, 39, 10, pp. 3863-3874.

De Hoog, P.,Gamez, P., Driessen, W. L. & Reedijk, J. (2002). New polidentate and polynucleatingN- donor ligands from amines and 2,4,6-trichoro-1,3,5-triazine. *Tetrahedron Letters*, 43, 38, pp. 6783-6786.

Dumont, R. S. (2013). Effects of charging and polarization on molecular conduction via the source-sink potential method. *Canadian Journal of Chemistry,* 92, 2, pp. 100-111.

Ekennia, A. C., Osowole, A. A., Olasunkanmi, L. O., Onwudiwe, D. C., Olubiyi, O. O. & Ebenso, E. E. (2017). Synthesis, characterization, DFT calculations and molecular docking studies of metal(II) complexes. *Journal of Molecular Structure*, 1150, pp. 279-292.

Ekennia, A. C., Osowole, A. A., Onwudiwe, D. C., Babahan, I., Ibeji, C. U., Okafor, S. N.& Ujam, O. T. (2018). *Appllied Organometallic Chemistry,* 32, 5, pp. e4310.

Fei, B., Yan, P., Liu, T., Yang, F. & Li, G. (2016). Synthesis and NIR luminescene of a series of salentype erbium complexes. *Journal of lumininescence*,177, pp. 380-386.

Feng, X., Wu, K. Y., Xie, S. Y., Li, R. –F. & Wang, L. –Y. (2017). A hetero metallic polymerbased on bis-salicylidene Schiff base ligand, synthesis, electronic chemistry, and antibacterial property. *Journal of Inorganic and Nano-Metal Chemistry*, 47, 8, pp. 1134-1140.

Frisch, M., Trucks, G., Schlegel, H. B., Scuseria, G., Robb, M., Cheeseman, J., Scalmani, G., Barone, V., Mennucci, B. & Petersson, G. (2009). Gaussian 09, revision D. 01, Gaussian, Inc., Wallingford CT

Gembicky, M., Boca, R. & Renz, F. (2000). A Heptanuclear Fe(III)-Fe(III)6 System with Twelve Unpaired Electrons. *Inorganic Chemistry Communications*, 3, pp. 662-665.

Gopalakrishnan, A. M. & Kumar, N. (2015). Antimalarial Action of Artesunate Involves DNA Damage Mediated by Reactive Oxygen Species. *Antimicrobial Agents and chemotherapy*, 59, 1, pp. 317- 325.

Gorller-Walrand, C. & Binnemans, K. (1998). *Spectral intensities of f–f transitions. In:Gschneidner Jr KA,Eyring L (Eds.), Handbook on the Physics Chemistry of Rare Earths.* North-Holland Publishers, Amsterdam, 25, pp. 101–264.

Hu, X., Castro-Rodriguez, I. & Meyer, K, (2003). Copper complexes of nitrogen – anchored tripodal N-heterocyclic carbene ligands. *Journal of American Chemical Society*,125, 40, pp. 12237 – 12245.

Ibeji, C. U., Adejoro, I. A. & Adeleke, B. B. (2015). A Benchmark Study on the Properties of Unsubstituted and Some Substituted Polypyrroles. *Journal of Physical Chemistry and Biophysics*, 5, 193, pp. 2161-0398.1000193.

Ibeji, C. U., Tolufashe, G. F., Ntombela, T., Govender, T., Maguire, G. E., Lamichhane, G., Kruger, H. G. & Honarparvar, B. (2018). The catalytic role of water in the binding site of L, D-transpeptidase 2 within acylation

mechanism: A QM/MM (ONIOM) modeling. *Tuberculosis*, 113, pp. 222-230.

Irie, R., Noda, K., Ito, Y., Matsumoto, N. & Katsuki, T. (1990). Catalytic asymmetric epoxidation of unfunctionalized olefins. *Tetrahedron Letters*, 31, 50, pp. 7345- 7348.

Kadhum, M. Y. (2011). Synthesis, identification and study of some new Schiff bases as inhibitors of brass corrosion and bacterial growth. *Journal of Basrah Researches (Sci.)*, 37, 2A, pp. 87 – 112.

Karatas, E. & Ucan, H. I. (2014). The Synthesis and characterization of s-triazine- based 8-hydroxyquinoline ligand and its salen/salophen-bridged Fe/Cr(III) capped complexes. *Journal of Selcuk University Natural and Applied Sci*ences, 3, 2, pp. 59-70.

Koc, Z. E. & Ucan, H. I. (2007). Complexes of iron(III) salen and saloph Schiff bases with bridging 2,4,6-tris(2,5-dicarboxyphenylmino-4-formylphenoxy)-1,3,5-triazine and 2,4,6-Tris(4-carboxyphenylimino-4^1-formylphenoxy)-1,3,5-triazine. *Transition Metal Chemistry*, 32. 5, pp. 597-602.

Kocyigit, O. (2013). A novel Schiff base bearing dopamine groups with tripodal

structure. Synthesis and its salen/salophen-bridged Fe/Cr(III) capped complexes. *Journal of Molecular Structure*, 1034. pp. 69-74.

Kocyigit, O. & Guler, E, (2010). The investigation of complexation properties and synthesis of the (salen and salophen) – bridged Fe/Cr (III) capped complexes of novel Schiff bases. *Journal of Inclusion Phenomena and Macrocyclic Chemistry*, 67, 1-2, 29-37.

Kopel, P., Sindelar, Z., Klicka, R. (1998). Complexes of Iron(III) Salen and Saloph Schiff Bases with Bridging Dicarboxylic and Tricarboxylic Acids. *Transition Metal Chemistry*, 23, pp. 139-142

Kostova, I., Manolov, I., Momekov, G. (2004). Cytotoxic activity of new neodymium(III) complexes of bis-coumarins. *European Journal of Medicinal Chemistry*, 39, 9, pp. 765-775.

Kostova, I., Manolov, I., Momekov, G., Tzanova, T., Konstantinov, S. & Karaivanova, M. (2005). Cytotoxic activity of new cerium(III) complexes of bis-coumarins. *European Journal of Medicinal Chemistry*, 40, 12, pp. 1246-1254.

Kumar, R., Gupta, L., Pal, P., Khan, S., Singh, N., Katiyar, S. B., Meena, S., Sarkar, J., Sinha, S., Kanaujiya, J. K., Lochab, S., Trivedi, A. K. & Chauhan, P. M. S. (2010). Synthesis and cytotoxicity evaluation of (tetrahydro-β-carboline)-1, 3, 5-triazine hybrids as anticancer agents. *European Journal of Medicinal Chemistry*,45(6): 2265-2276.

Lawal, M. M., Govender, T., Maguire, G. E., Honarparvar, B. & Kruger, H. G. (2016). Mechanistic Investigation of the Uncatalyzed Esterification Reaction of Acetic Acid and Acid Halides With Methanol: A DFT Study. *Journal of Molecular Modelling*, 22, 10, pp. 235.

Lemke, T. L., Williams, D. A., Roche, V. F. to, S. W. (2010). *Foye's Principles of Medicinal Chemistry 6th ed.* Wolters Kluwer PvtLtd, New Delhi. pp. 438 - 440.

Lekha, L., Raja, K. K., Rajagopal, G. & Easwaramoorthy, D. (2014). Synthesis, spectroscopic characterization and antibacterial studies of lanthanide (III) Schiff base complexes containing N, O donor atoms. *Journal of Molecular Structure*, 1056 – 1057, pp. 307-313.

Lorke, D. (1983). A new approach to tropical acute toxicity testing. Arch Toxicology, 53, 4, pp. 275-287

Manolov, I., Kostova, I., Konstantinov, S. & Karaivanova, M. (1999). Synthesis, physicochemical characterisation and cytotoxic screening of new complexes of cerium, lanthanum and neodymium with warfarin and coumachlor sodium salts.

European Journal of Medicinal Chemistry, 34. 10, pp. 853-858.

Milata, V., Reinprecht, L. & Kizlink, J. (2012). Synthesis and Antifungal efficacy of 1,3,5-triazines. *Acta Chimica Slovaca,* 5, 1, pp. 55-99

Mohanan, K., Devi, S. N. & Murukan, B. (2006). Complexes of copper(II) with 2-(N-Salicylideneamino)-3-carboxyethyl-4,5,6,7-tetrahydrobenzo[b]thiophene containing different counter anions. *Synthesis and Reactivity in Inorganic, Metal-Organic, and Nano-Metal Chemistry,* 36, 6, pp. 441 – 449.

Morris, G. M., Huey, R., Lindstrom, W., Sanner, M. F., Belew, R. K., Goodsell, D. S. & Olson, A. J. (2009). AutoDock4 and AutoDockTools4: Automated docking with selective receptor flexibility. *Journal of Computational Chemistry,* 30, 16, pp. 2785-2791.

Oakley, A. J. (2010). The structure of Aspergillus niger phytase PhyA in complex with a phytate mimetic. *Biochemistry Biophysics Research Communications,* 397, 4, pp. 745-749.

Obasi, L. N., Oruma, U. S., Al-Swaidan, I. A., Ramasami, P., Ezeorah, C. J. & Ochonogor, A. E. (2017). Synthesis, characterization and antibacterial studies of N-(Benzothiazol-2-yl)-4-chlorobenzenesulphonamide and its neodymium(III) and thallium(III) complexes. *Molecules*, 22, 153, pp. 1-11.

Olanrewaju, A. A., Ibeji, C. U. & Fabiyi, F. S. (2018). Synthesis, Characterization and computational studies of metal(II) complexes derived from β-diketone and Para-aminobenzoic acid. *Indian J ournal of Heterocyclic Chemistry,* 28(3): 351-361.

Oruma, U. S., Ukoha, P. O. & Asegbeloyin, J. N. (2014). Synthesis, characterization and biological studies of S-1,3-benzothiazol-2-ylthiophene-2-carbothioate and its Ce(IV) and Nd(III) complexes. *Asian Journal of Chemistry,*26, 22, pp. 7622-7626.

Peter, W., Portus, H. & Robinson, L. (1975). The Four Day Suppressive *In Vivo* Anti-malarial Test. *Annals of Tropical. Medicine and Parasitology*, 69, pp. 155-171.

Rauf, S. M. A., Arvidsson, P. I., Albericio, F., Govender, T., Maguire, G. E., Kruger, H. G. & Honarparvar, B. (2015). The effect of N-methylation of amino acids (Ac-X-OMe) on solubility and onformation: a DFT study. *Organic and Biomolecular Chemistry* 13, 39, pp. 9993-10006.

Runge, E., Gross, E. K. U. (1984). Density-functional theory for time dependent systems. *Physical. Reviews and Letters*, 52, 12, pp, 997-1000.

Saczewski, F., Bulakowska, A., Bednarski, P. & Grunert, R. (2006). Synthesis, structure and anticancer activity of novel 2,4-diamino-1,3,5-triazine derivatives. *European Journal of Medicinal Chemistry*, 41, 2, pp. 219-22.

Saidu, K., Onah, J., Orisadipe, A., Olusola, A., Wambebe, C. & Gamaliel, K. (2000). Antiplasmodial, analgesic and anti-inflammmatory activities of aqueous extract of *Erythrinasenegalensis*. *Journal of Ethnopharmacology*, 71, 1-2, pp. 275-280.

Sanner, M. F. (1999). Python: a programming language for software integration and development. *Journal of Mol Graph Model* 17(1): 57-61.

Sathe, G. B., Vaidya, V. V., Deshmukh, R. G., Kekare, M. B., Kulkarni, V. S., Chasker, A. C. (2013). Synthesis of novel C2-symmetric salen molecules. *Journal of Applicable Chemistry,* 2. 3, pp. 433- 437.

Silverstein, R. M., Webster, F. X., Kiemle, D. J. (2005). *Spectrometric identification of organic compounds, edn. 7.* John wiley& Sons, Inc, Hoboken. Pp. 106, 153, 200, 228.

Suendo, V. & Viridi, S. (2011). Ab initio calculation of UV-Vis absorption spectra of a single molecule chlorophyll a: Comparison study between RHF/CIS, TDDFT, and semi-empirical methods. *arXiv preprint arXiv* 1105, pp. 3766.

Taha, Z. A., Ajlouni, A. M., Al-Hassan, K. A., Hajazi, A. K. & Faiq, A. B. (2011). Synthesis, characterization, biological activity and fluorescence properties of bis-(salicylaldehyde)-1,3-propylenediimine schiff base ligand and its lanthanide complexes. *Spectrochimica Acta*, Part A 81, 1, pp. 317-323

Tahmassebi, D. C. & Sasaki, T. (1994). Synthesis of a new trialdehyde template for molecular imprinting. *Journal of Organometallic Chemistry*, 59. 3, pp. 679-681.

Ukwe, C. V., Epueke, E. A., Ekwunife, O. I., Okoye, T. C., Akudor, G. C., Ubaka, C. M. (2010). Antimalarial activity of aqueous extract and fractions of leaves of*Ageratumconyziodes*in mice infected with *Plasmodium berghei*. *International Journal of Pharmaceutical Sciences*, 2, 1, pp. 33-38

Uysal. S. & Ucan, H. I. (2009a). The Synthesis and characterization of melamine based Schiff bases and its trinuclear [salen/salophenFe(III)] and [salen/salophenCr(III)] capped complexes. *Journal of Inclusion Phenomena and Macrocyclic Chemistry*, 65, 3-4, pp. 299-304.

Uysal, S. & Ucan, H. I. (2009b). The Synthesis and characterization of 2,4,6-tris(3,4-dihydroxybenzimino)-1,3.5-triazine and its [salen/salophenFe(III)] and salen/salophenCr(III)] capped complexes. *Journal of Inclusion Phenomena and Macrocyclic Chemistry*, 65, 3-4, pp. 403-409.

Uysal, S., Koc, Z. E., Celikbilek, S., Ucan, H. I. (2012). Synthesis of star-shaped macromolecular Schiff base complexes having melamine cores and their magnetic and thermal behaviours. *Synthetic Communications*, 42, 7, pp. 1033-1044.

Uysal, S. & Koc, Z. E. (2016). Synthesis and characterization of dopamine substituetripodaltrinuclear [(salen/salophen/salpropen) M] (M = Cr(III), Mn(III), Fe(III) ions) capped S-triazine complexes: Investigation of their thermal and magnetic properties. *Journal of Molecular Structure*, 1109, pp. 119-126.

Uysal, S. & Koc, Z. E. (2010). Synthesis and characterization of dendrimeric melamine cored [salen/salophenFe(III)] and [salen/salophenCr(III)] capped complexes and their magnetic behaviors. *Journal of Hazardous Materials*, 175, 1-3, pp. 532-539.

Wolters, K. (2009), *Clinical Pharmacology made incredibly easy-3rd edition.* W and Wilkins, Lippincott, USA, pp. 285 – 286, 239 – 256.

Yang, B., Hao, F., Li, J., Chen, D., Liu, R. (2013). Binding of chrysoidine to catalase: spectroscopy, isothermal titration calorimetry and molecular docking *studies. Journal of Photochemistry and Photobiology B*, 128, pp. 35-42.

Yue, Y., Yan, P., Sun, J., Hou, G. & Li, G. (2015). Structure and luminescent properties of 2D salen-type lanthanide coordination polymers from the flexible N,N[1]-bis(salicylidene)-1,4-butanediamine ligand. *Polyhedron***,** 94, pp. 90-95.

Zhang, W., Loebach, J. L., Wilson, S. R., Jacobsen, E. N. (1990). Enantioselective epoxidation of unfunctionalized olefins catalyzed by salen manganese complexes. *Journal of American Chemical Society*, 112, 7, pp. 2801-2803.

Zheng, M., Xu, C., Ma, J., Sun, Y., Du, F., Liu, H., Lin, L., Li, C., Ding, J., Chen, K. & Jiang, H. (2007). Synthesis and antitumor evaluation of a novel series of triaminotriazineanalogs. *Bioorganic and Medicinal Chemistry*, 15, 4, pp. 1815-1827.

Conflict of interests

The authors declare that there is no conflict of interests regarding the publication of this paper and are responsible for the contents and writing of the paper. The authors have filed a patent application for the synthesis of $[\{Dy/Er(salen)\}_3(H_3CT)]^{3+}\cdot 3H_2O$.